

Characterization of NiO-TiO₂ Modified with WO₃ and Catalytic Activity for Acid Catalysis

Young Il Pae,[†] Mu Hee Bae, Won Cheon Park, and Jong Rack Sohn*

Department of Applied Chemistry, Engineering College, Kyungpook National University, Daegu 702-701, Korea

[†]Department of Chemistry, University of Ulsan, Ulsan 680-749, Korea

Received August 27, 2004

A series of NiO-TiO₂/WO₃ catalysts was prepared by drying powdered Ni(OH)₂-Ti(OH)₄ with ammonium metatungstate aqueous solution, followed by calcining in air at high temperature. Characterization of prepared catalysts was performed by using FTIR, Raman, XPS, XRD, and DSC and by measuring surface area. Upon the addition of tungsten oxide to titania up to 25 wt%, the specific surface area and acidity of catalysts increased in proportion to the tungsten oxide content due to the interaction between tungsten oxide and titania. Since the TiO₂ stabilizes the tungsten oxide species, for the samples equal to or less than 25 wt%, tungsten oxide was well dispersed on the surface of titania, but for the samples containing above 25 wt%, the triclinic phase of WO₃ was observed at calcination temperature above 400 °C. The catalytic activities of 10-NiO-TiO₂/WO₃ for 2-propanol dehydration and cumene dealkylation were correlated with the acidity of catalysts measured by ammonia chemisorption method. NiO may attract reactants and enhance the local concentration of reactants near the acid sites, consequently showing the increased catalytic activities.

Key Words : NiO-TiO₂/WO₃ catalyst, Characterization, Acid catalysis, 2-Propanol dehydration, Cumene dealkylation

Introduction

Supported metal oxides¹⁻³ exhibit interesting catalytic behavior depending on the kind of support, the content of active component, and the preparation method. It is well known that the dispersion, the oxidation state, and the structural features of supported species may strongly depend on the support. Structure and physicochemical properties of supported metal oxides are considered to be different compared with bulk metal oxides because of their interaction with supports.

On the other hand, solid acid catalysts play an important role in hydrocarbon conversion reactions in the chemical and petroleum industries.^{4,5} Many kinds of solid acids have been found, their acidic properties on catalyst surfaces, their catalytic action, and the structure of acid sites have been elucidated for a long time, and those results have been reviewed by Arata.⁶ The strong acidity of zirconia-supported sulfate has attracted much attention because of its ability to catalyze many reactions such as cracking, alkylation, and isomerization. The potential for a heterogeneous catalyst has yielded many papers on the catalytic activity of sulfated zirconia materials.⁶⁻⁸ Sulfated zirconia incorporation Fe and Mn has been shown to be highly active for butane isomerization, catalyzing the reaction even at room temperature.⁹⁻¹¹ Coelho *et al.*¹² have discovered that the addition of Ni to sulfated zirconia causes an activity enhancement comparable to that caused by the addition of Fe and Mn.

It has been reported by several workers that the addition of

platinum to zirconia modified by sulfate ions enhances catalytic activity in the skeletal isomerization of alkanes without deactivation when the reaction is carried out in the presence of hydrogen.^{13,14} The high catalytic activity and small deactivation can be explained by both the elimination of the coke by hydrogenation and hydrogenolysis,¹³ and the formation of Brønsted acid sites from H₂ on the catalysts.¹⁴ Recently, Hino and Arata reported zirconia-supported tungsten oxide as an alternative material in reaction requiring strong acid sites.^{6,15} Several advantages of tungstate, over sulfate, as a dopant include that it does not suffer from dopant loss during thermal treatment and it undergoes significantly less deactivation during catalytic reaction.¹⁶

So far, however, supported tungsten oxide catalysts have been studied mainly on alumina, silica and zirconia,¹⁷⁻²³ and little work was studied for the binary oxide support, NiO-TiO₂. This paper describes the characterization of NiO-TiO₂ modified with WO₃ and catalytic activity for acid catalysis. The characterization of the samples was performed by means of Fourier transform infrared (FTIR), X-ray diffraction (XRD), X-ray photoelectron spectra (XPS), Raman spectroscopy, and the measurement of surface area. For the acid catalysis, the 2-propanol dehydration and cumene dealkylation were used as test reactions.

Experimental Section

Catalyst Preparation. The coprecipitate of Ni(OH)₂-Ti(OH)₄ was obtained by adding aqueous ammonia slowly into a mixed aqueous solution of nickel chloride and titanium tetrachloride at 100 °C with stirring until the pH of mother liquor reached about 8. The coprecipitate thus

*To whom correspondence should be addressed. e-mail: jrsohn@knu.ac.kr

obtained was washed thoroughly with distilled water until chloride ion was not detected, and was dried at room temperature for 12 h. The dried precipitate was powdered below 100 mesh.

The catalysts containing various tungsten oxide contents were prepared by adding an aqueous solution of ammonium metatungstate $[(\text{NH}_4)_6(\text{H}_2\text{W}_{12}\text{O}_{40})\cdot n\text{H}_2\text{O}]$ to the $\text{Ni}(\text{OH})_2\text{-Ti}(\text{OH})_4$ powder followed by drying and calcining at high temperatures for 1.5 h in air. This series of catalysts are denoted by their weight percentage of NiO and WO_3 . For example, 10-NiO-TiO₂/15-WO₃ indicates the catalyst containing 10 wt % NiO regarding only two components, NiO and TiO₂, and containing 15 wt % WO₃ regarding all three components, NiO, TiO₂ and WO₃.

Characterization. FTIR spectra were obtained in a heatable gas cell at room temperature using Mattson Model GL6030E spectrophotometer. The self-supporting catalyst wafers contained about 9 mg/cm². Prior to obtaining the spectra the sample were heated under vacuum at 400-500 °C for 1.5 h.

The Raman spectra were recorded on a Spex Ramalog spectrometer with holographic gratings. The 5145-Å line from a Spectra-Physics Model 165 argon-ion laser was used as the exciting source. The spectral shift width was typically 4 cm⁻¹, and laser source powers of approximately 45 mW, measured at the sample, were used.

X-ray photoelectron spectra was obtained with a VG scientific model ESCALAB MK-11 spectrometer. Al K_α and Mg K_α were used as the excitation source, usually at 12 kV, 20 mA. The analysis chamber was at 10⁻⁹ torr or better and the spectra of sample, as fine powder, were analyzed. Binding energies were referenced to the C_{1s} level of the adventitious carbon at 285.0 eV

Catalysts were checked in order to determine the structure of the support as well as that of tungsten oxide by means of a Jeol Model JDX-8030 diffractometer, employing Cu K_α (Ni-filtered) radiation.

DSC measurements were performed by a PL-STA model 1500H apparatus in air, and the heating rate was 5 °C per minute. For each experiment 10-15 mg of sample was used.

The specific surface area was determined by applying the BET method to the adsorption of N₂ at -196 °C. Chemisorption of ammonia was also employed as a measure of the acidity of catalysts. The amount of chemisorption was determined based on the irreversible adsorption of ammonia.²⁴⁻²⁶

Results and Discussion

Raman and Infrared Spectra. The Raman spectra of WO₃ obtained by calcining ammonium metatungstate at 500 °C, 25-NiO-TiO₂/30-WO₃, 25-NiO-TiO₂/15-WO₃, 25-NiO-TiO₂/5-WO₃, and TiO₂ under ambient conditions are presented in Figure 1. The WO₃ structure is made up distorted WO₃ octahedra. The major vibrational modes of WO₃ are located at 808, 714, and 276 cm⁻¹, and have been assigned to the W=O stretching mode, the W=O bending

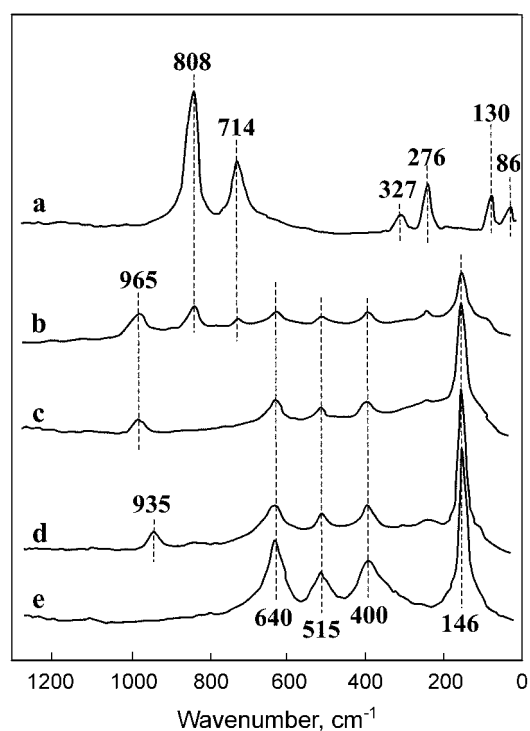


Figure 1. Raman spectra of (a) WO₃, (b) 25-NiO-TiO₂/30-WO₃, (c) 25-NiO-TiO₂/15-WO₃, (d) 25-NiO-TiO₂/5-WO₃, and (e) TiO₂.

mode, and the W-O-W deformation mode, respectively.²⁷ The Raman spectrum of the 25-NiO-TiO₂/5-WO₃ sample shows a weak and broad band at ~935 cm⁻¹ which is characteristic of tetrahedrally coordinated surface tungsten oxide species.²⁸ This assignment is in agreement with the WO₃/γ-Al₂O₃ system where combined Raman and XANES data revealed the presence of distorted tetrahedral coordination at low loading.²⁹ In addition to this 935 cm⁻¹ band, the feature of titania at 640, 515, 400, and 146 cm⁻¹ is also present. These Raman bands have been assigned to the anatase modification,³⁰ which is in agreement with the results of XRD described later.

The molecular structures of the supported tungsten oxide species also are found to depend on the loading. As the loading is increased, the W=O stretching modes shifts upward to 965 cm⁻¹. The 965 cm⁻¹ band in the Raman spectrum of the 25-NiO-TiO₂/15-WO₃ sample is assigned to the octahedrally coordinated polytungstate species.²⁸ The shift from 935 cm⁻¹ for 25-NiO-TiO₂/5-WO₃ to 965 cm⁻¹ for 25-NiO-TiO₂/15-WO₃ is in agreement with reported Raman spectra,²⁸ and suggest that under ambient conditions different two-dimensional tungsten oxide species may be present in the NiO-TiO₂/WO₃ samples. At 30% loading three bands also appear in the Raman spectrum at 808, 714, and 276 cm⁻¹, showing the presence of crystalline WO₃³¹ in addition to the two-dimensional tungsten oxide species (band at 965 cm⁻¹). These results are in good agreement with those of XRD. That is, for 25-NiO-TiO₂/5-WO₃ sample the crystalline WO₃ phase was not observed, while for 25-NiO-TiO₂/30-WO₃ sample the triclinic phase of crystalline WO₃ appeared at the calcination temperature of 400-800 °C. It

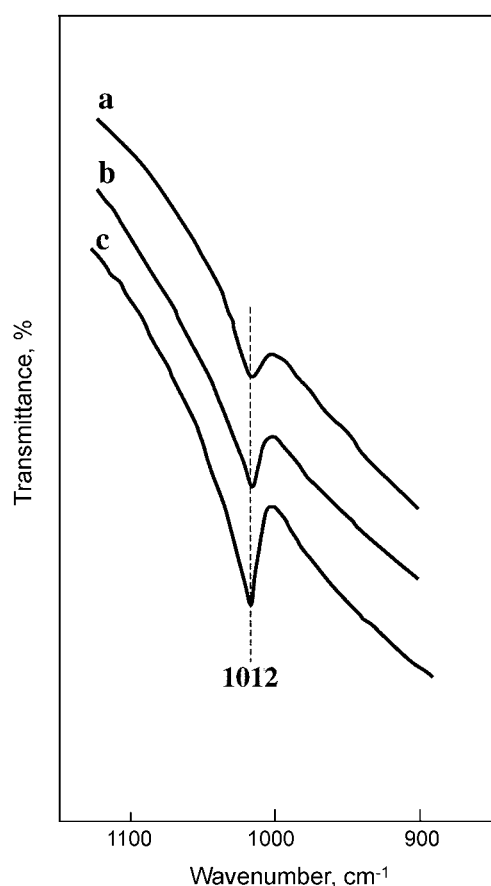


Figure 2. Infrared spectra of (a) 25-NiO-TiO₂/5-WO₃, (b) 25-NiO-TiO₂/15-WO₃, and (c) 25-NiO-TiO₂/25-WO₃ evacuated at 500 °C for 1 h.

seems likely that for 25-NiO-TiO₂/30-WO₃, monolayer coverage has been exceeded and WO₃ crystals are also present on the surface.

Raman spectra above was recorded under ambient conditions. To examine the structure of tungsten oxide complex under dehydration conditions, IR spectra of NiO-TiO₂/WO₃ samples were obtained in a heatable gas cell after evacuation at 500 °C for 1 h. The in situ IR spectra for 25-NiO-TiO₂/WO₃ having different WO₃ contents are presented for the range 1100-900 cm⁻¹ in Figure 2. The IR single band at 1012 cm⁻¹ is due to the symmetrical W=O stretching mode of the tungsten oxide complex coordinated to the NiO-TiO₂ surface. The same results have been obtained at the other samples. This shows that the dehydration changes the molecular structures and that the two-dimensional tetrahedrally coordinated tungsten oxide species as well as the octahedrally coordinated polytungstate species are converted into the same highly distorted octahedrally coordinated structure as proposed for the WO₃/TiO₂ system by Wachs *et al.*²⁸ The 1012 cm⁻¹ IR band matches the Raman absorption at 1015 cm⁻¹.²⁸ For the 25-NiO-TiO₂/WO₃ samples evacuated at 500 °C, as shown in Figure 2, the band intensity at 1012 cm⁻¹ increases with increasing the WO₃ content, indicating that the higher the WO₃ content, the more the octahedrally coordinated WO₃ species.

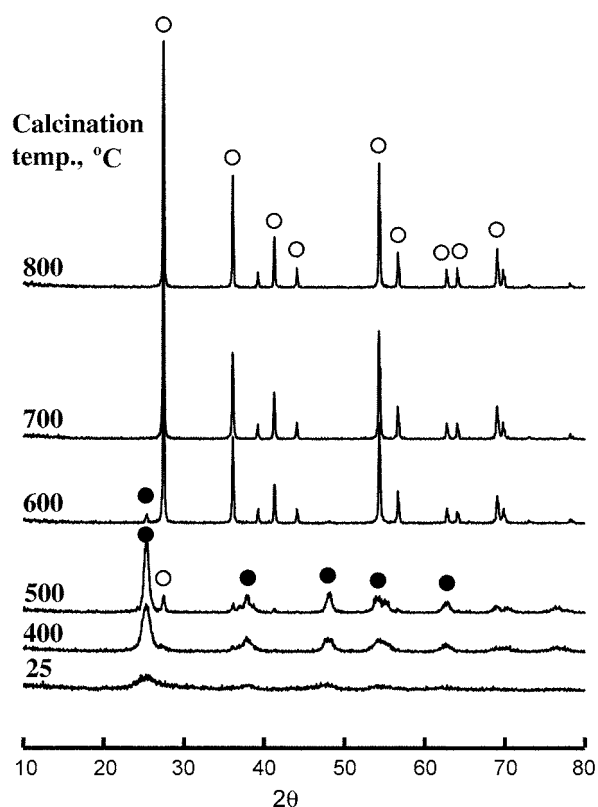


Figure 3. X-ray diffraction patterns of TiO₂ calcined at different temperature for 1.5 h: ●, anatase TiO₂; ○, rutile TiO₂.

Crystalline Structures of Catalysts. The crystalline structures of TiO₂ and NiO-TiO₂/WO₃ calcined in air at different temperatures for 1.5 h were examined. As shown in Figure 3, TiO₂ was amorphous to X-ray diffraction at 25 °C, with an anatase phase at 400 °C, a two-phase mixture of the anatase and rutile forms at 500 °C, and a rutile phase at 600-800 °C.

However, in the case of NiO-TiO₂/WO₃ catalysts the crystalline structures of samples were different from that of support, TiO₂. For the 5-NiO-TiO₂/15-WO₃, as shown in Figure 4, TiO₂ is anatase phase up to 700 °C. However, from 600 °C nickel titanium oxide (NiTiO₃) was observed due to the reaction between TiO₂ and NiO and its amount increased with increasing calcination temperature. X-ray diffraction data indicated a two-phase mixture of the anatase and rutile TiO₂ forms at 800 °C. It is assumed that the interaction between tungsten oxide and TiO₂ hinders the transition of TiO₂ from anatase to rutile phase.³²⁻³⁴ The presence of tungsten oxide strongly influences the development of textural properties with temperature in comparison with pure TiO₂. No phase of tungsten oxide was observed up to 25 wt % at any calcination temperature, indicating a good dispersion of tungsten oxide on the surface of TiO₂ support due to the interaction between them. Moreover, for the samples of 5-NiO-TiO₂/15-WO₃ and 25-NiO-TiO₂/15-WO₃ the transition temperature from the anatase to rutile phase was higher by 200 °C, than that of pure TiO₂. As shown in Figure 5, for 25-NiO-TiO₂/15-WO₃ TiO₂ was amorphous to

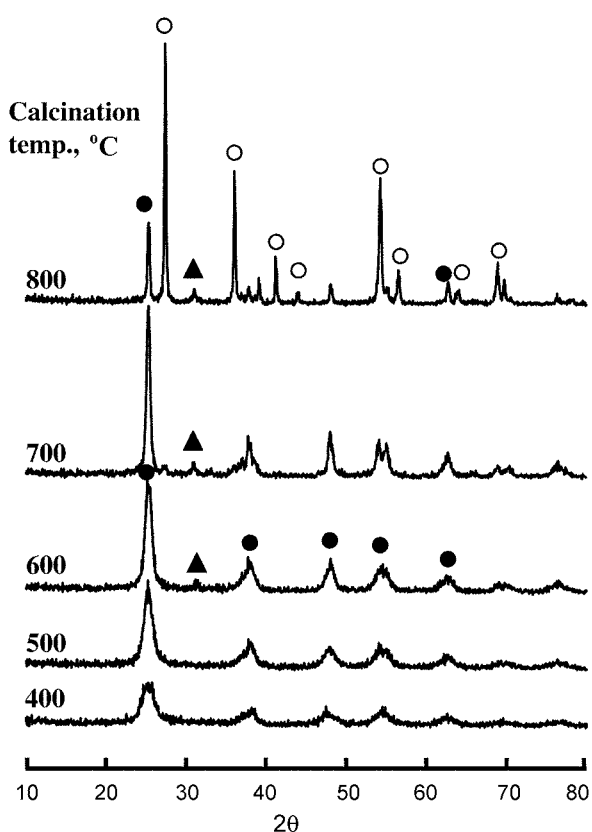


Figure 4. X-ray diffraction patterns of 5-NiO-TiO₂/15-WO₃ calcined at different temperature for 1.5 h: ●, anatase TiO₂; ○, rutile TiO₂; ▲, NiTiO₃.

X-ray diffraction up to 400 °C, with a anatase phase of TiO₂ at 500-650 °C, a two-phase mixture of the anatase and rutile TiO₂ forms at 700 °C, and rutile TiO₂ forms at 800 °C. Nickel titanium oxide was also observed at 600-800 °C, showing the increased amount with the calcination temperature. However, for 25-NiO-TiO₂/30-WO₃ sample triclinic phase of crystalline WO₃ due to the decomposition of ammonium metatungstate was observed in the samples calcined at 400-800 °C (not shown in the figure).

X-ray Photoelectron Spectra. Interactions with a support can dramatically change the properties metals or metal oxides.³⁵ Figure 6 shows the W 4f spectra of some NiO-TiO₂/WO₃ samples containing different tungsten oxide content and calcined at 500 °C. The W 4f_{7/2} binding energy measured for NiO-TiO₂/WO₃ samples occurred at 36 eV and corresponds to tungsten in the +6 oxidation state (WO₃).³⁶ Generally, the spectrum of supported WO₃ is broader than that of WO₃ due to the interaction between the WO₃ and support. It is known that there is a very strong interaction between WO₃ and Al₂O₃ so that tungsten oxide species is present as W⁺⁶ after calcination of WO₃/Al₂O₃ sample. As shown in Figure 6, for 25-NiO-TiO₂/WO₃ samples calcined in air tungsten oxide species are present as W⁺⁶, indicating the strong interaction between WO₃ and NiO-TiO₂. For 25-NiO-TiO₂/30-WO₃, it seems likely that above monolayer coverage crystalline WO₃ exists on the surface of TiO₂ and

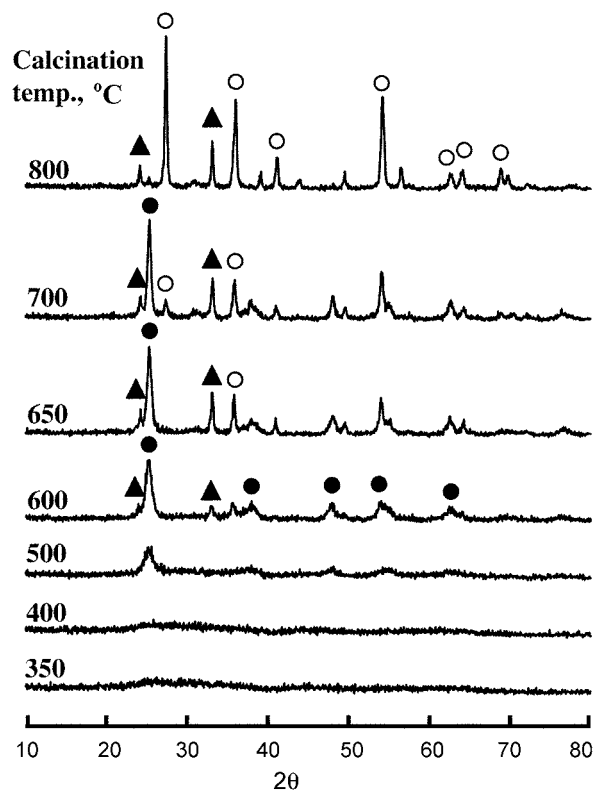


Figure 5. X-ray diffraction patterns of 25-NiO-TiO₂/15-WO₃ calcined at different temperature for 1.5 h: ●, anatase TiO₂; ○, rutile TiO₂; ▲, NiTiO₃.

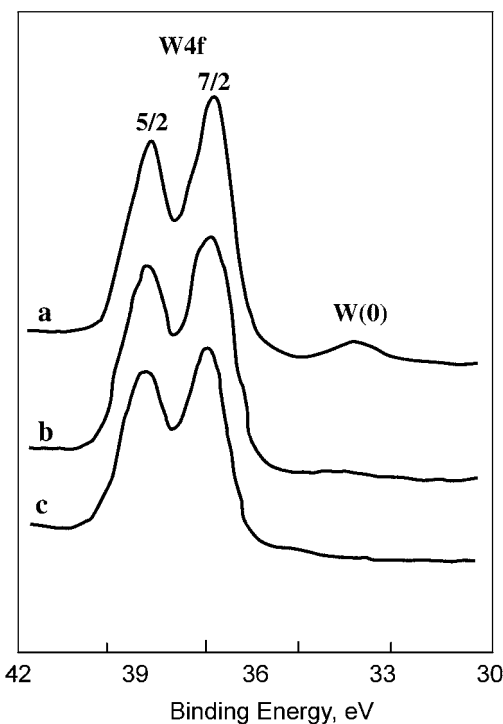


Figure 6. W_{4f} XPS of (a) 25-NiO-TiO₂/30-WO₃, (b) 25-NiO-TiO₂/15-WO₃, and (c) 25-NiO-TiO₂/5-WO₃.

well can be reduced to metallic W during calcination.²⁸

Thermal Analysis. In X-ray diffraction pattern, it was

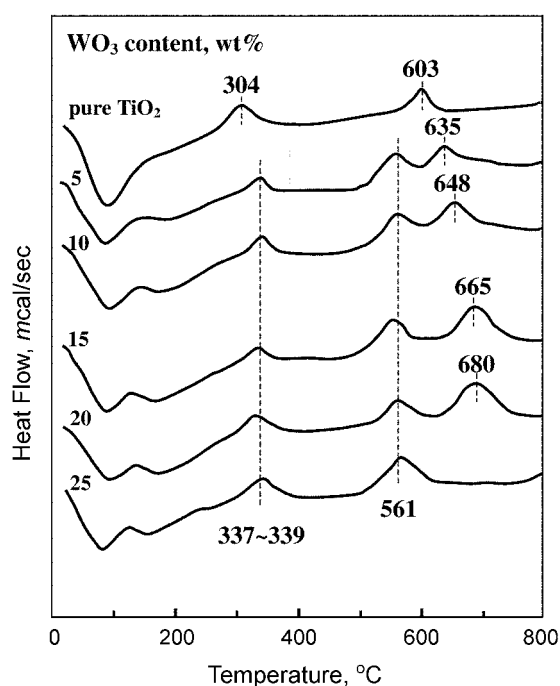


Figure 7. DSC curves of precursors for TiO₂ and 25-NiO-TiO₂/WO₃ having different WO₃ contents.

shown that the structure of NiO-TiO₂/WO₃ was different depending on the calcined temperature. To examine the thermal properties for the precursors of samples more clearly, their thermal analysis was carried out (Figure 7). For pure TiO₂ the DSC curve showed a broad endothermic peak around 100 °C due to water elimination, and two exothermic peaks at 303 and 602 °C due to the phase transition of TiO₂ from amorphous to anatase, and from anatase to rutile, respectively.³⁴ In the case of NiO-TiO₂/WO₃ a broad endothermic peak appeared around 170 °C is due to the evolution of NH₃ and H₂O decomposed from ammonium metatungstate, and an exothermic peak at 561 °C is due to the NiTiO₃ formation from NiO and TiO₂. However, it is of interest to see the influence of WO₃ on the crystallization of TiO₂ from amorphous to anatase phase, and phase transition of TiO₂ from anatase to rutile. As shown in Figure 7, the exothermic peak due to the phase transition of TiO₂ appeared at 302 °C for pure TiO₂, while for NiO-TiO₂/WO₃ it was shifted to

Table 1. Specific surface area and acidity of 10-NiO-TiO₂/WO₃ catalysts containing different WO₃ contents and calcined at 400 °C for 1.5 h

WO ₃ content (wt %)	Surface area (m ² /g)	Acid amount (μmol/g)
0 (TiO ₂)	72	78
5	310	216
10	316	221
15	315	229
20	315	238
25	314	249
30	287	167

Table 2. Specific surface area and acidity of NiO-TiO₂/15-WO₃ catalysts containing different NiO contents and calcined at 400 °C for 1.5 h

NiO content (wt %)	Surface area (m ² /g)	Acid amount (μmol/g)
5	267	199
10	316	222
15	318	226
20	320	233
25	323	234
30	317	213
40	312	202

higher temperatures, 337-379 °C. The exothermic peak due to the phase transition from anatase to rutile appeared at 603 °C for pure TiO₂, while for 25-NiO-TiO₂/WO₃ the shift to higher temperature increased with increasing WO₃ content up to 20 wt % of WO₃. It is considered that the interaction between WO₃ and TiO₂ delays the transition of TiO₂ from amorphous to anatase phase and from anatase to rutile phase.³²⁻³⁴ These results are in agreement with those of X-ray diffraction patterns described above.

Surface Properties. It is necessary to examine the effect of tungsten oxide and nickel oxide on the surface properties of catalysts, that is, specific surface area, acidity, and acid strength. The specific surface area and acidity 10-NiO-TiO₂/WO₃ having different WO₃ contents and calcined at 400 °C for 1.5 h are listed in Table 1. The presence of tungsten oxide strongly influences the surface area and acidity in comparison with the pure TiO₂. Specific surface area and acidity of 10-NiO-TiO₂/WO₃ samples are much larger than that of pure TiO₂ calcined at the same temperature, showing that surface area and acidity increase gradually with increasing tungsten oxide content up to 25 wt % of WO₃. It seems likely that the interaction between tungsten oxide and TiO₂ not only protects catalysts from sintering, but increase the acidity due to the double bond nature of the W=O described below.

In addition to tungsten oxide content, we examined the effect of NiO on the surface area and acidity values. The surface area and acidity of NiO-TiO₂/25-WO₃ having different NiO contents and calcined at 400 °C for 1.5 h are listed in Table 2. Unlike WO₃, NiO did not influence both surface area and acidity values, indicating that NiO does not make new acid sites.

The acid strength of the catalysts was examined by a color change method, using Hammett indicator^{32,33} in sulphuryl chloride. 5-NiO-TiO₂/15-WO₃ sample after enacuation at 500 °C for 1 h was estimated to have H₀ ≤ -14.5, indicating the formation of superacidic sites. Since it was very difficult to observe the color of indicators adsorbed on the catalyst of high nickel oxide content, the low percentage of nickel oxide (5 wt %) was used in this experiment. Acids stronger than H₀ ≤ -11.93, which corresponds to the acid strength of 100% H₂SO₄, are superacids.³⁶ Consequently, NiO-TiO₂/WO₃ catalysts would be solid superacids. The superacidic

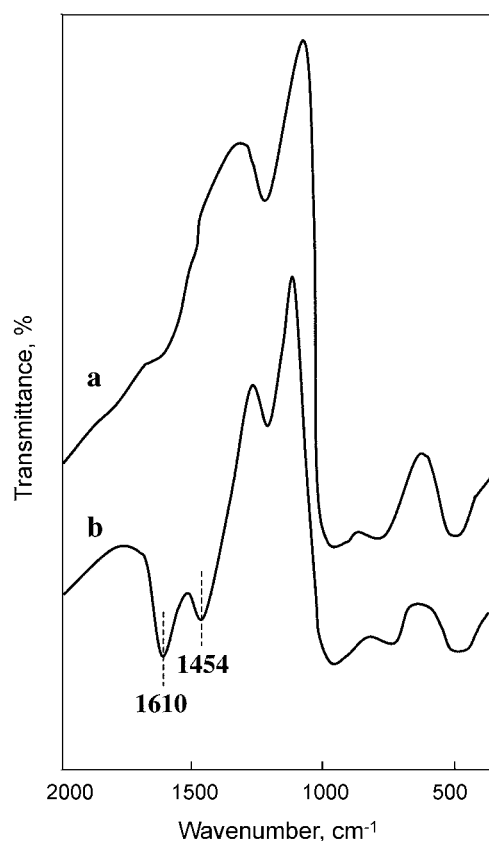


Figure 8. Infrared spectra of NH_3 adsorbed on 20-NiO-TiO₂/15-WO₃: (a) background of 20-NiO-TiO₂/15-WO₃ evacuated at 500 °C for 1 h; (b) ammonia (20 Torr) adsorbed on (a); gas phase was evacuated at 230 °C for 1 h.

property is attributed to the double bond nature of the W=O in the complex formed by the interaction of TiO₂ with tungstate, in analogy with the case of ZrO₂ modified with chromate and sulfate ion.^{33,37,38}

Infrared spectroscopic studies of ammonia adsorbed on solid surfaces have made it possible to distinguish between Brønsted and Lewis acid sites.³⁹⁻⁴¹ Figure 8 shows the IR spectra of ammonia adsorbed on 25-NiO-TiO₂/15-WO₃ sample evacuated at 500 °C for 1 h. The band at 1454 is the characteristic peak of ammonium ion, which is formed on the Brønsted acid sites and the absorption peak at 1610 cm⁻¹ is contributed by ammonia coordinately bonded to Lewis acid sites,³⁹⁻⁴¹ indicating the presence of both Brønsted and Lewis acid sites on the surface of 25-NiO-TiO₂/15-WO₃ sample. Other samples having different WO₃ and NiO contents also showed the presence of both Lewis and Brønsted acids.

Catalytic Activities for Acid Catalysis. It is interesting to examine how the catalytic activity of acid catalyst depends on the acid property. For both 2-propanol dehydration and cumene dealkylation reactions NiO-TiO₂/WO₃ catalysts calcined at 400 °C exhibited the highest catalytic activities. So, after this, emphasis has been placed on the catalysts calcined at 400 °C. The catalytic activity of 10-NiO-TiO₂/WO₃ for the 2-propanol dehydration is measured and the

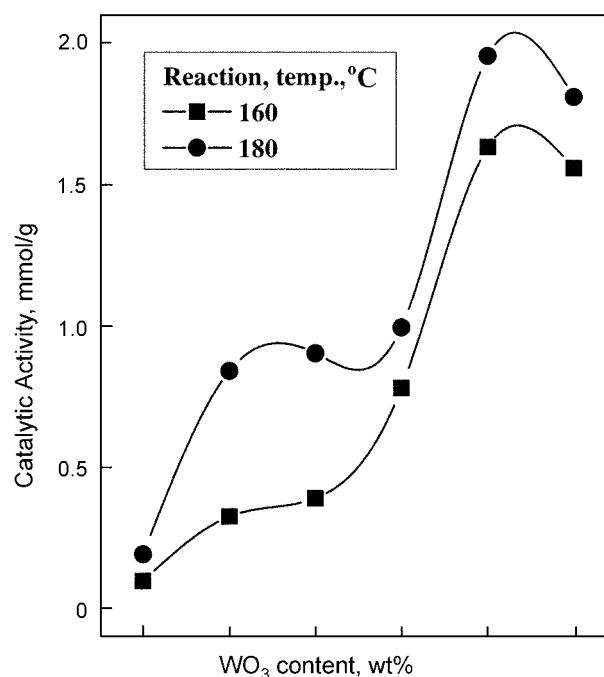


Figure 9. Catalytic activity of 10-NiO-TiO₂/WO₃ for 2-propanol dehydration as a function of WO₃ content.

results are illustrated as a function of WO₃ content in Figure 9, where reaction temperature is 160-180 °C. In view of Table 1 and Figure 9, the variation in catalytic activity for 2-propanol dehydration is correlated with the change of their acidity, showing the highest activity and acidity for 10-NiO-TiO₂/25-WO₃. It has been known that 2-propanol dehydration takes place very readily on weak acid sites.^{42,43} Good correlations have been found in many cases between the acidity and the catalytic activities of solid acids. For example, the rates of both the catalytic decomposition of cumene and the polymerization of propylene over SiO₂-Al₂O₃ catalysts were found to increase with increasing acid amounts at strength $H_0 \leq +3.3$.⁴⁴ The catalytic activities for both reactions, 2-propanol dehydration and cumene dealkylation, were correlated with the acidity of NiSO₄ supported on TiO₂-ZrO₂ measured by an ammonia chemisorption method. It was also reported that the catalytic activity of nickel silicates in the ethylene dimerization as well as in the butene isomerization was closely correlated with the acid amount of the catalyst.⁴⁵

Cumene dealkylation takes place on relatively strong acid sites of the catalysts.^{42,43,46} Catalytic activity for cumene dealkylation against WO₃ content is presented in Figure 10, where reaction temperature is 400-450 °C. Comparing Table 1 and Figure 10, the catalytic activity is also correlated with the acidity. The correlation between catalytic activity and acidity holds for both reactions, cumene dealkylation and 2-propanol dehydration, although the acid strength required to catalyze acid reaction is different depending on the type of reactions.^{42,43} As seen in Figures 9 and 10, the catalytic activity for cumene dealkylation, in spite of higher reaction temperature, is lower than that for 2-propanol dehydration.

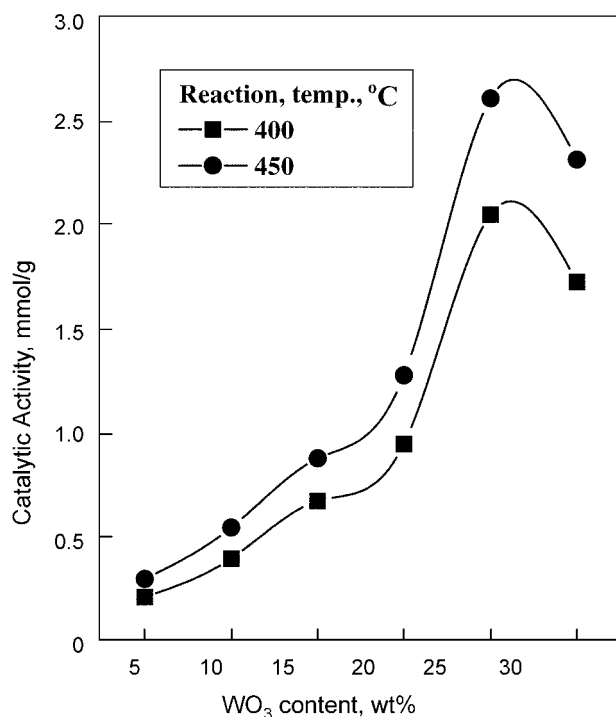


Figure 10. Catalytic activity of 10-NiO-TiO₂/WO₃ for cumene dealkylation as a function of WO₃ content.

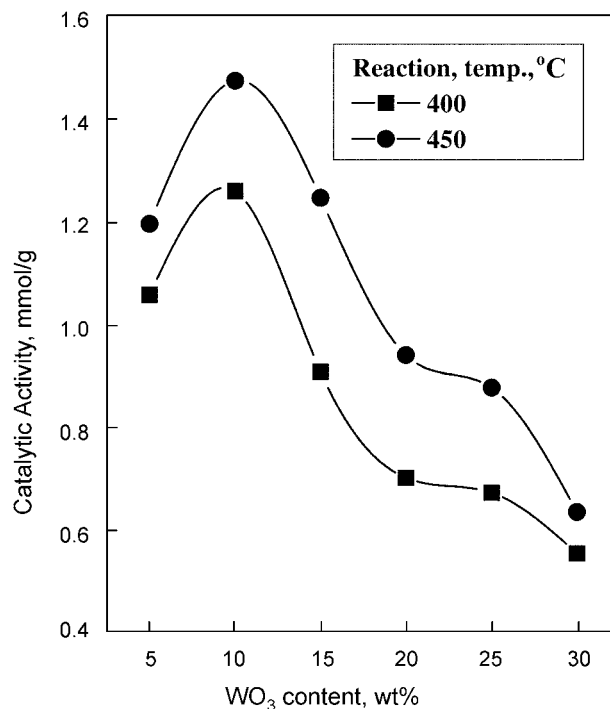


Figure 12. Catalytic activity of NiO-TiO₂/15-WO₃ for cumene dealkylation as a function of NiO content.

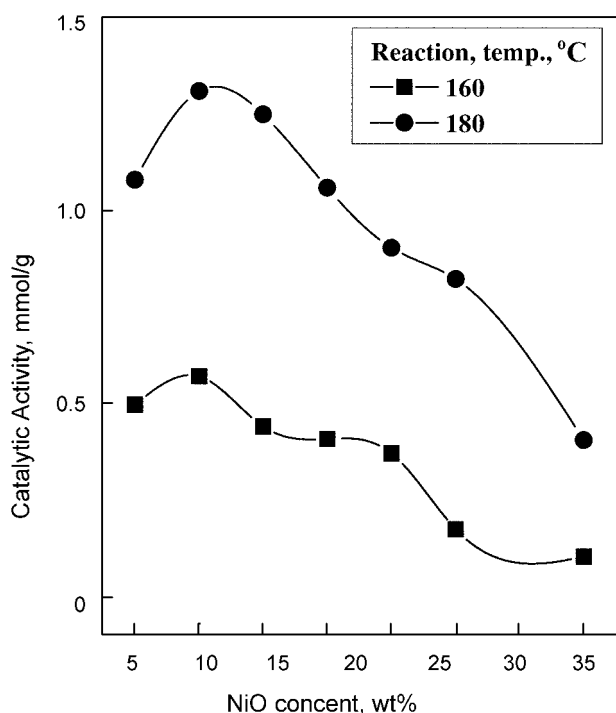


Figure 11. Catalytic activity of NiO-TiO₂/15-WO₃ for 2-propanol dehydration as a function of NiO content.

To examine the promoting effect of NiO on the catalytic activities, the catalytic activities of NiO-TiO₂/15-WO₃ for 2-propanol dehydration and cumene dealkylation are plotted as a function of NiO in Figures 11 and 12, respectively. For both reactions the catalytic activities increased with increas-

ing NiO content up to 10 wt% and then decreased. However, in view of Table 2 and Figures 11 and 12, the increases of catalytic activities by the addition of NiO seem not to be correlated with the acidity of catalysts, because the addition of NiO did not bring about the increase of acidity as listed in Table 2. So, it is very important to examine the role of NiO for acid catalysis. According to the hypothesis of Coelho *et al.*,¹² for sulfated zirconia by addition of metal promoters the high n-butane isomerization activity was explained in terms of a bifunctional mechanism in which the metal promoters are responsible for an increase in the surface concentration of olefins rather than an increased acidity. We might suggest an alternative hypothesis, which is closely related to that postulated by Coelho *et al.*¹² We might propose that the presence of NiO may attract reactants and enhance the local concentration of reactants near the acid sites, consequently showing the increased catalytic activities.

Conclusions

A series of NiO-TiO₂/WO₃ catalysts was prepared by adding an aqueous solution of ammonium metatungstate to the Ni(OH)₂-Ti(OH)₄ powder followed by drying and calcining at high temperatures for 1.5 h in air. The interaction between tungsten oxide and titania influences the physicochemical properties of prepared catalysts with calcination temperature. Since the TiO₂ stabilizes the surface tungsten oxide species, for the samples equal to or less than 25 wt%, tungsten oxide will be dispersed on the surface of titania, but for the samples above 25 wt% the triclinic phase of WO₃ was observed at any calcination temperature. The acidity of

10-NiO-TiO₂/WO₃ increased with increasing WO₃ content up to 25 wt%, showing the presence of Brönsted and Lewis acid sites on the surface of catalyst. The high acid strength and acidity are responsible for the W=O bond nature of complex formed by the interaction between WO₃ and TiO₂. The catalytic activities of 10-NiO-TiO₂/WO₃ catalysts for 2-propanol dehydration and cumene dealkylation were correlated to their acidity. It is proposed that NiO may attract reactants and enhance the local concentration of reactants near the acid sites, consequently showing the increased catalytic activities.

Acknowledgements. This work was supported by 2003 Research Fund of University of Ulsan and was partially supported by grant No. (R05-2003-000-10074-0) from the Basic Research Program of the Korea Science Engineering Foundation. We wish to thank Korea Basic Science Institute for the use of Laman and X-ray Instruments.

References

- Wainwright, M. S.; Foster, N. R. *Catal. Rev.* **1979**, *19*, 211.
- Dadyburjor, D. B.; Jewur, S. S.; Ruckenstein, E. *Catal. Rev.* **1979**, *19*, 293.
- Sohn, J. R. *J. Ind. Eng. Chem.* **2004**, *10*, 1.
- Cheung, T. K.; d'Itri, J. L.; Lange, F. C.; Gates, B. C. *Catal. Lett.* **1995**, *31*, 153.
- Tanabe, K.; Misono, M.; Ono, Y.; Hattori, H. *New Solid Acids and Bases*; Elsevier Science: Amsterdam, 1989; Chapter 4.
- Arata, K. *Adv. Catal.* **1990**, *37*, 165.
- Ward, D. A.; Ko, E. I. *J. Catal.* **1994**, *150*, 18.
- Kustov, L. M.; Kazansky, V. B.; Figueras, F.; Tichit, D. *J. Catal.* **1994**, *150*, 143.
- Hsu, C. Y.; Heimbuch, C. R.; Armes, C. T.; Gates, B. C. *J. Chem. Soc., Chem. Commun.* **1992**, 1645.
- Hosoi, T.; Shimadzu, T.; Ito, S.; Baba, S.; Takaoka, H.; Imai, T.; Yokoyama, N. *Prepr. Symp. Div. Petr. Chem.*; American Chemical Society: Los Angeles, CA, 1988; p 562.
- Ebitani, K.; Konishi, J.; Hattori, H. *J. Catal.* **1991**, *130*, 257.
- Coelho, M. A.; Resasco, D. E.; Sikabwe, E. C.; White, R. L. *Catal. Lett.* **1995**, *32*, 253.
- Lange, F. C.; Cheung, T. K.; Gates, B. C. *Catal. Lett.* **1994**, *41*, 95.
- Zarkalis, S.; Hsu, C. Y.; Gates, B. C. *Catal. Lett. Commun.* **1994**, *29*, 235.
- Hino, M.; Arata, K. *J. Chem. Soc., Chem. Commun.* **1987**, 1259.
- Larsen, G.; Lotero, E.; Parra, R. D. In *Proceeding of the 11th International Congress on Catalysis*; Elsevier: New York, 1996; pp 543-551.
- Basrur, A. G.; Patwardham, S. R.; Vyas, S. N. *J. Catal.* **1991**, *127*, 86.
- Roosnaiern, A. J.; Koster, D.; Moi, J. C. *J. Phys. Chem.* **1980**, *84*, 3075.
- Karakonstantis, L.; Bourikas, K.; Lycourghiotis, A. *J. Catal.* **1996**, *162*, 295.
- Grunert, W.; Shpiro, E. S.; Feldhaus, R.; Anders, K.; Antoshin, G. V.; Minachev, K. M. *J. Catal.* **1987**, *107*, 522.
- Santesteban, J. R.; Vartuli, J. C.; Han, S.; Bastian, R. D.; Chang, C. D. *J. Catal.* **1997**, *168*, 431.
- Boyse, R. A.; Ko, E. I. *J. Catal.* **1997**, *171*, 191.
- Sohn, J. R.; Park, M. Y. *J. Ind. Eng. Chem.* **1998**, *4*, 84.
- Sohn, J. R.; Lee, S. H.; Park, W. C.; Kim, H. W. *Bull. Korean Chem. Soc.* **2004**, *25*, 657.
- Sohn, J. R.; Seo, D. H.; Lee, S. H. *J. Ind. Eng. Chem.* **2004**, *10*, 309.
- Sohn, J. R.; Lee, S. H. *Appl. Catal. A: General* **2004**, *266*, 89.
- Anderson, A. *Spectrosc. Lett.* **1976**, *9*, 809.
- Vuurman, M. A.; Wach, I. E.; Hirt, A. M. *J. Phys. Chem.* **1991**, *95*, 9928.
- Horsley, J. A.; Wachs, I. E.; Brown, J. M.; Via, G. H.; Hardcastle, F. D. *J. Phys. Chem.* **1987**, *91*, 4014.
- Engweiler, J.; Harf, J.; Baiker, A. *J. Catal.* **1996**, *159*, 259.
- Chan, S. S.; Wachs, I. E.; Murrel, L. L. *J. Catal.* **1984**, *90*, 150.
- Sohn, J. R.; Cho, S. G.; Pae, Y. I.; Hayashi, S. *J. Catal.* **1996**, *159*, 170.
- Sohn, J. R.; Ryu, S. G. *Langmuir* **1993**, *9*, 126.
- Sohn, J. R.; Bae, J. H. *Korean J. Chem. Eng.* **2000**, *17*, 86.
- Tauster, S. J.; Fung, S. C.; Baker, R. T. K.; Horsley, J. A. *Science* **1981**, *211*, 1121.
- Olah, F. G. A.; Prakash, G. K. S.; Sommer, J. *Science* **1979**, *206*, 13.
- Sohn, J. R.; Kim, H. J. *J. Catal.* **1986**, *101*, 428.
- Sohn, J. R.; Kim, H. W. *J. Mol. Catal.* **1989**, *52*, 361.
- Basila, M. R.; Kantner, T. R. *J. Phys. Chem.* **1967**, *71*, 467.
- Satsuma, A.; Hattori, A.; Mizutani, K.; Furuta, A.; Miyamoto, A.; Hattori, T.; Murakami, Y. *J. Phys. Chem.* **1988**, *92*, 6052.
- Sohn, J. R.; Park, W. C. *Appl. Catal. A: General* **2003**, *239*, 269.
- Sohn, J. R.; Jang, H. J. *J. Mol. Catal.* **1991**, *64*, 349.
- Decanio, S. J.; Sohn, J. R.; Paul, P. O.; Lunsford, J. H. *J. Catal.* **1986**, *101*, 132.
- Tanabe, K. *Solid Acids and Bases*; Kodansha: Tokyo, 1970; p 103.
- Sohn, J. R.; Ozaki, A. *J. Catal.* **1980**, *61*, 29.
- Sohn, J. R.; Chun, E. W.; Pae, Y. I. *Bull. Korean Chem. Soc.* **2003**, *24*, 1785.